

Pressure and temperature dependence of the Fano resonance in the Raman spectrum of $A_2\text{FeMoO}_6$ systems ($A=\text{Sr}, \text{Ca}$)

D. Marrocchelli,¹ P. Postorino,¹ D. Di Castro,¹ E. Arcangeletti,¹ P. Dore,¹ M. Cestelli Guidi,² Sugata Ray,^{3,4,5} and D. D. Sarma^{3,5}

¹“Coherencia” CNR-INFN and Dipartimento di Fisica, Università di Roma La Sapienza, Piazzale Aldo Moro 2, I-00185 Roma, Italy

²Laboratori Nazionali di Frascati-INFN, Via E. Fermi 40, 00044 Frascati, Italy

³Solid State and Structural Chemistry Unit, Indian Institute of Science, Bangalore 560012, India

⁴Department of Material Science, Indian Association for the Cultivation of Science, Kolkata 700032, India

⁵Centre for Advanced Materials, Indian Association for the Cultivation of Science, Kolkata 700032, India

(Received 1 April 2007; revised manuscript received 28 September 2007; published 8 November 2007)

We report on Raman measurements carried out on $\text{Ca}_2\text{FeMoO}_6$ and $\text{Sr}_2\text{FeMoO}_6$ double perovskites as functions of pressure (0–15 GPa) and of temperature (298–370 K). The Raman spectrum of both the samples is characterized by a phonon peak at $\sim 460\text{ cm}^{-1}$ whose large asymmetric profile is ascribed to a Fano resonance. The careful data analysis provides in particular the Fano asymmetry parameter q which results to be nearly independent from pressure and temperature, thus suggesting a remarkable stability of both charge-carrier density and charge-lattice coupling. Finally, our data allow us to ascribe the conductivity transition previously observed around 2 GPa in $\text{Sr}_2\text{FeMoO}_6$ not to an intrinsic property but to the pressure-induced opening of intergrain percolation paths.

DOI: [10.1103/PhysRevB.76.172405](https://doi.org/10.1103/PhysRevB.76.172405)

PACS number(s): 75.30.-m, 62.50.+p, 78.30.-j, 75.47.-m

Double perovskite systems ($A_2\text{FeMoO}_6$ with $A=\text{Ca}, \text{Sr}, \text{Ba}$) have recently attracted a large interest^{1,2} because of the high spin polarization of charge carriers below the Curie temperature T_C which makes these materials good candidates for many technological applications.³ The great advantage which the $A_2\text{FeMoO}_6$ compounds have over other systems which show spin-polarized conductivity [e.g., manganites such as $\text{La}_{1-x}\text{Ca}_x\text{MnO}_3$ (Ref. 4)] is that the half-metallic state is achieved in undoped samples at room temperature since T_C in these systems can be much higher than ambient temperature.^{1,2}

The ideal crystal structure of $A_2\text{FeMoO}_6$ compounds is that of an ordered ABO_3 perovskite where Fe and Mo ions have alternate occupancies at the B site.⁵ At ambient conditions, the ideal cubic structure is shown by the $\text{Ba}_2\text{FeMoO}_6$ system only since slight distortions occur as the A -ion size decreases: $\text{Sr}_2\text{FeMoO}_6$ and $\text{Ca}_2\text{FeMoO}_6$ show tetragonal and monoclinic structures, respectively.⁵ Below T_C , the $A_2\text{FeMoO}_6$ systems become ferrimagnetic with a magnetization value per unit cell close to $4\mu_B$ as a result of the antiferromagnetic coupling between Fe^{3+} ($S=5/2$) and Mo^{5+} ($S=1/2$) sublattices.² Spin-polarized conductivity below T_C is thus explained by density of states calculations^{1,2} which show that the electrons of Mo and Fe ions can be considered as localized and itinerant, respectively. A magnetic mechanism based on the large hopping between Fe and Mo via the O ion, is responsible for the high T_C values of these systems.⁶ In this framework, no important role was attributed to electron-lattice coupling.²

Although the theoretical framework appears to be rather well assessed,^{6,7} recent experimental results open questions about the possible interplay among lattice, electronic, and spin degrees of freedom and call for a deeper understanding of the physics of these systems. A first issue arises from recent Raman measurements on $\text{Sr}_2\text{FeMoO}_6$ at ambient conditions, where the asymmetric profile of a phonon peak was

ascribed to a Fano resonance, thus implying the presence of charge-lattice coupling.⁸ A second issue is focused on rather contrasting results about the effect of the loss of magnetic order on the conduction regime of these systems. On one hand, electrical conductivity measurements on $\text{Ba}_2\text{FeMoO}_6$ show a transition from a metal-like to a semiconductorlike conductivity regime on increasing the temperature above T_C .⁹ On the other hand, infrared measurements carried out on $\text{Sr}_2\text{FeMoO}_6$ do not show significant variation in the low energy optical conductivity on crossing T_C .¹⁰ Finally, several polycrystalline compounds of the $\text{Sr}_{2-x}\text{Ba}_x\text{FeMoO}_6$ family show an abrupt drop of the electrical resistance around 2 GPa particularly remarkable for $\text{Sr}_2\text{FeMoO}_6$ (about 6 order of magnitude).^{11,12} This phenomenon does not appear to be connected to modification of the structure, which instead is very stable over a wide pressure range.^{11,12}

The presence of a Fano resonance^{13,14} in the phonon spectrum makes Raman spectroscopy an ideal tool for investigating these systems. Indeed, temperature and pressure dependences of the electron-phonon coupling and of the charge-carrier density can be inferred by means of a careful analysis of the resonant phonon line shape.¹⁴ In the present Brief Report, we report on Raman measurements of $\text{Sr}_2\text{FeMoO}_6$ (SFMO) and $\text{Ca}_2\text{FeMoO}_6$ (CFMO) carried out as functions of temperature and pressure. Additional infrared (IR) measurements were also performed on CFMO at ambient pressure as a function of temperature.

Polycrystalline samples of SFMO and CFMO were prepared by a standard method of solid state reaction.¹⁵ Magnetic measurements provided $T_C=370$ and 315 K for SFMO and CFMO, respectively.¹⁶ Raman measurements were carried out using a confocal micro-Raman spectrometer (Infinity by Jobin-Yvon) equipped with a He-Ne laser source and a 1800 g/cm grating. The notch filter used to reject the elastic contribution of the backscattered light prevented low-frequency measurements; spectra were collected in the

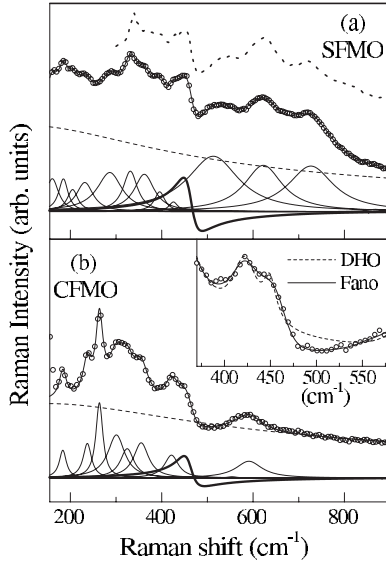


FIG. 1. Room temperature Raman spectra (circles) and best-fit curves (continuous lines) for SFMO (panel a) and CFMO (panel b) are shown. The electronic (dashed line), DHO (full line), and Fano (bold line) best-fit components are also shown. The Raman spectrum of SFMO from Ref. 8 is shown in panel (a) for the sake of comparison. Inset: best-fit curves obtained with and without the inclusion of a Fano profile compared with the CFMO spectrum.

150–1000 cm^{-1} frequency range. The laser beam was focused by a long distance $20\times$ objective into a spot of about $5\ \mu\text{m}$ diameter at the sample surface. The diamond anvil cell (DAC) used in high-pressure experiments was equipped with $800\ \mu\text{m}$ culet IIA diamonds and filled with sample grains with up to $10\ \mu\text{m}$ across and NaCl used as pressure transmitting medium. Further experimental details and procedures are reported in Ref. 17. Midinfrared (MIR) reflectivity spectra within the $600\text{--}5000\ \text{cm}^{-1}$ spectral range were collected by means of a Cassegrain-based infrared microscope coupled to a Michelson interferometer (Bruker Equinox 55). The reflectance spectrum $R(\omega)$ of the sample was obtained through measurements on a reference gold surface.

Raman spectra measured at room temperature and ambient pressure on SFMO and CFMO are shown in Figs. 1(a) and 1(b), respectively. The present SFMO spectrum is in good agreement with previous Raman data from a polycrystalline bulk sample⁸ [see Fig. 1(a)]. In Ref. 8, an assignment of the Raman phonon peaks was also proposed exploiting the results of a polarization analysis of the Raman response of highly oriented SFMO films. In particular, the phonon line at around $460\ \text{cm}^{-1}$ was ascribed to a B_g mode and its strongly asymmetric profile to the effect of a Fano resonance.⁸ To our knowledge, no Raman spectra were previously reported for CFMO, and it is worth noticing that, also in this case, an asymmetric phonon line at around $460\ \text{cm}^{-1}$ is observed [see Fig. 1(b)]. The Raman spectra were at first fitted using a standard model curve¹⁸ given by a linear combination of damped harmonic oscillator (DHO) for the phononic contributions plus an electronic background,

$$[1 + n(\omega)] \left(\frac{B\omega\Gamma}{\omega^2 + \Gamma^2} + \sum_{i=1}^N \frac{A_i \gamma_i^2 \omega_i \omega}{(\omega_i^2 - \omega^2)^2 + \gamma_i^2 \omega_i^2} \right). \quad (1)$$

The parameters B and Γ characterize the electronic response and ω_i , γ_i , and A_i are frequency, linewidth, and intensity of the i -th phonon mode, respectively. The quantity $[1 + n(\omega)]$ accounts for the Bose-Einstein statistics. We found for both the samples that a full agreement between the best-fit curves and the measured spectra is obtained only when a Fano profile,¹⁹

$$\frac{A_F \gamma_F [\gamma_F \omega^2 \cos \theta - (\omega_F^2 - \omega^2) \omega \sin \theta]}{(\omega_F^2 - \omega^2)^2 + \gamma_F^2 \omega^2}, \quad (2)$$

instead of a simple DHO is used to describe the asymmetric phonon lines of SFMO and CFMO (see the inset of Fig. 1 for CFMO). In Eq. (2), the additional parameter θ determines the line asymmetry and it is usually discussed in terms of the Fano asymmetry parameter $q = 1/\tan(\theta/2)$ (i.e., a DHO is obtained for $q \rightarrow \infty$ which corresponds to $\theta = 0$). Best-fit electronic, DHO, and Fano components are shown separately in Figs. 1(a) and 1(b). As to the Fano components, best-fit parameter values show that the peak frequencies are the same in both samples ($463 \pm 3\ \text{cm}^{-1}$ in agreement with previous results on SFMO [Ref. 8]) as well as the q values ($q = -1.4 \pm 0.3$ in SFMO and $q = -1.3 \pm 0.3$ in CFMO).

We chose CFMO ($T_C \approx 315\ \text{K}$) for temperature-dependent measurements aimed at investigating possible spectroscopic signature of the magnetic transition. Raman spectra collected on increasing temperature from 300 to $365\ \text{K}$ are shown in Fig. 2. The data do not show remarkable anomalies on crossing T_C ; a weak continuous softening of the phonon frequencies and an overall broadening of the spectral features are observed. The variations observed in the relative intensities of the phonon peaks can be ascribed to thermal and polarization effects. The latter is due to the thermal expansion of the sample holder which causes small displacements of the polarized laser beam on the sample surface thus moving the impinged area from crystallite to crystallite. On increasing the temperature, best-fit results confirm the phonon softening (e.g., the most intense structure goes from $264\ \text{cm}^{-1}$ at room temperature to $256\ \text{cm}^{-1}$ at $365\ \text{K}$) and show that the ratio of the integrated intensities of the electronic background over the overall phonon spectrum does not significantly vary and that the q parameter remains nearly constant within estimated uncertainties, as shown in the inset of Fig. 2(a).

MIR reflectivity measurements carried out on CFMO within the same temperature range show that the reflectance spectrum $R(\omega)$ does not significantly change on crossing T_C [see the inset of Fig. 2(b)]. The low-frequency crossing of the two $R(\omega)$ [see Fig. 2(b)] might be ascribed to a temperature-dependent reduction of the phonon impurity scattering, although we notice that the maximum difference observed is very close to the experimental uncertainty. Present reflectivity measurements together with those previously collected on SFMO (Ref. 10) strongly support the ab-

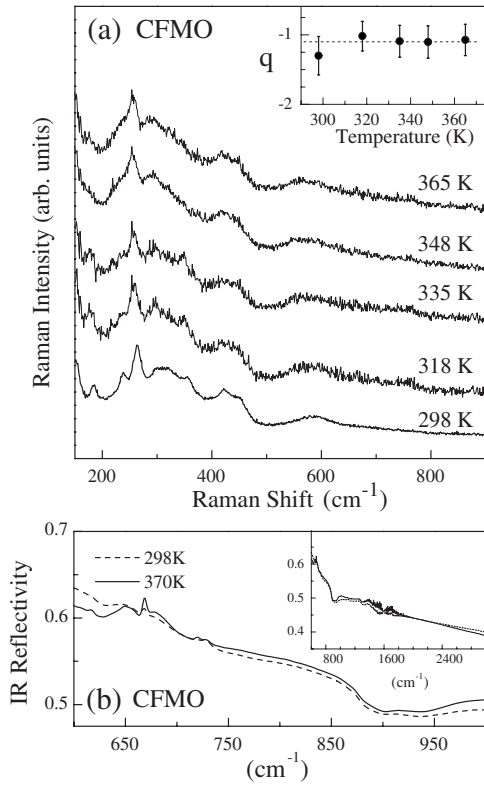


FIG. 2. (a) Raman spectra of CFMO at different temperatures. Inset: temperature dependence of the asymmetry parameter q , the horizontal line shows the weighted average value (-1.1 ± 0.2). (b) IR reflectivity $R(\omega)$ at 298 and 370 K over a low-frequency range and over the full measured range in the inset.

sence of a remarkable coupling between the magnetic ordering and the frequency-dependent conductivity which determines the $R(\omega)$ spectrum.

In order to investigate the role of the electron-phonon coupling revealed by the Fano resonance, we induced controlled volume compression by applying very high pressure on the samples. Room temperature Raman spectra of SFMO and CFMO were collected as a function of pressure up to 10.5 and 15.5 GPa, respectively. Raman spectra of the two compounds are shown in Fig. 3 at several selected pressures. Variation of the relative intensities of the phonon peaks can be mostly ascribed to polarization effects caused by pressure-induced reorientation of crystallite and micrometric misalignment of the laser beam on the sample surface after each pressure increase.

The data were analyzed by means of the same fitting procedures adopted above. However, when a weak Raman scatterer, such as CFMO and particularly SFMO, is investigated using a DAC, the contribution due to the diamond fluorescence is no more negligible. The measured fluorescence spectrum of the diamond window multiplied by a factor treated as a free fitting parameter was thus added to the model fitting curve. Best-fit components, including the diamond contribution, are shown in Fig. 3 at the highest pressure. Also in this case, best-fit parameters show that the intensity of both the electronic contribution and the overall phonon spectrum does not remarkably change with increas-

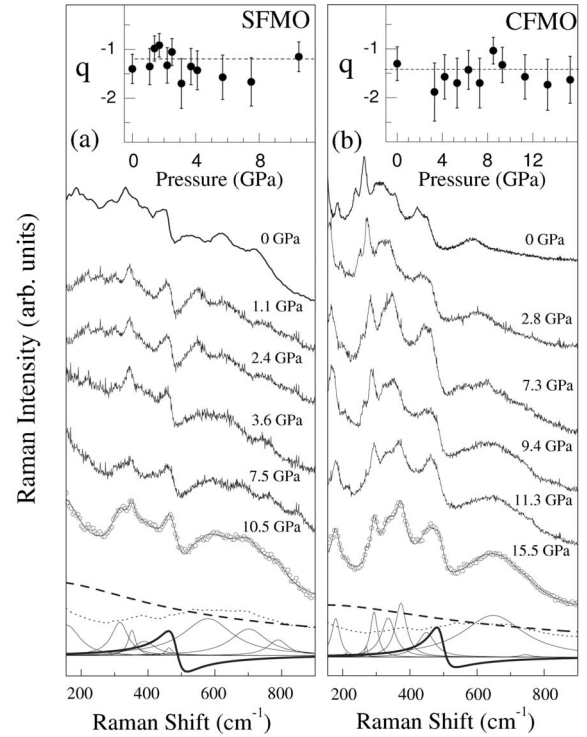


FIG. 3. Raman spectra of (a) SFMO and (b) CFMO at selected pressures. For the highest-pressure spectra, best-fit electronic (dashed lines), diamond background (dotted lines), DHO (full lines), and Fano (bold lines) components are shown separately. Insets: pressure dependence of the asymmetry parameter q , horizontal lines show the weighted average values (-1.4 ± 0.4 for CFMO and -1.2 ± 0.5 for SFMO).

ing pressure. A continuous pressure-induced phonon hardening (about $2 \text{ cm}^{-1}/\text{GPa}$) is observed for both the samples. In particular, the analysis of the Fano line shapes shows the same hardening rate ($2.1 \pm 0.2 \text{ cm}^{-1}/\text{GPa}$), and in both cases, the q parameters remain constant within estimated uncertainties, as shown in the insets of Fig. 3.

In discussing results obtained for the Fano asymmetry parameter q , it is worth recalling that, in a solid system, q can be expressed as¹⁴

$$q = \text{const} \frac{T_{ph}}{\rho T_{el} V_{el-ph}}, \quad (3)$$

where T_{el} and T_{ph} are the electron and phonon transition-matrix elements, respectively, ρ is the density of charge carriers, and V_{el-ph} is the electron-phonon interaction. Since the Raman intensity of both the overall phonon spectrum and the electronic contribution does not remarkably change on varying temperature and pressure, it is reasonable to assume that T_{el} and T_{ph} do not substantially change as well. Under this assumption, q depend on ρ and V_{el-ph} only at least over the temperature and pressure ranges explored.

The combined temperature-dependent Raman and MIR measurements on CFMO do not show any anomaly at T_C . In particular, over a temperature range around T_C , the stability of the asymmetry factor q indicates that the product ρV_{el-ph} is

nearly constant and the absence of detectable temperature variation in the reflectivity spectra suggests a stability of ρ . Combining the above findings, our spectroscopic analysis shows that the loss of magnetic order in CFMO does not affect neither the charge-carrier density nor the electron-phonon coupling. The absence of correlation between the magnetic transition and the optical properties can be extended to SFMO on the basis of previous temperature-dependent IR measurements.¹⁰ This suggests that the magnetoconductive transition observed in Ba₂FeMoO₆ around T_C (Ref. 9) is a peculiar characteristic of this system. However, it is worth noting that a change in conductivity as small as the one observed in Ba₂FeMoO₆ might be hardly detectable through optical measurements.

The high-pressure Raman study shows that q is nearly pressure independent in both CFMO and SFMO. By considering the high structural stability of SFMO up to very high pressures¹¹ and the absence of remarkable variation of the electronic background in the present measurements, it is reasonable to conclude that not only the product ρV_{el-ph} but also the single factors are nearly constant over the investigated pressure range. Bearing in mind the huge drop observed in the electrical resistance of SFMO around 2 GPa,¹¹ present results indicate that such effect should be ascribed not to an intrinsic property but to the pressure-induced opening of intergrain percolation paths. Indeed, this mechanism only can explain the pressure-induced drop of the resistance, since q , i.e., ρ and V_{el-ph} , do not significantly change on increasing pressure. Furthermore, it is worth noting that micro-Raman measurements can probe intrinsic single-grain properties, since the laser spot is smaller than the single grains. The importance of intergrain effects in transport measurements is evidenced by the magnetoresistance observed in polycrystalline SFMO samples,^{1,2} not in single crystals.²¹

In summary, the present Brief Report reports on a spec-

troscopic study of Sr₂FeMoO₆ and Ca₂FeMoO₆. High-pressure Raman measurements were carried out on both the samples over a wide pressure range (0–15 GPa), and additional Raman and infrared measurements were performed within a small temperature range around T_C . In reference with the issues reported in the opening paragraphs of the present Brief Report, the main results can be schematized as follow:

(i) The presence of a Fano resonance in the Raman spectrum was confirmed for Sr₂FeMoO₆ and observed in Ca₂FeMoO₆. The asymmetry parameter q was determined and its value found nearly the same in both compounds. The electron-phonon coupling revealed by the Fano resonance appears to be actually independent on both pressure and temperature over the investigated ranges.

(ii) No spectroscopic signatures of the magnetic transition were found. The loss of magnetic order does not affect neither the low-frequency-dependent conductivity nor the lattice dynamics.

(iii) The nearly constant q value obtained for both the samples over the whole pressure range rules out the possibility that the conductivity transition, previously observed at around 2 GPa, could be ascribed to an intrinsic mechanism but strongly suggests an intergrain percolation mechanism.

We want to finally note that the pressure independence of the asymmetry factor q , and thus also of the electron-phonon coupling, is a particularly interesting point when compared with the results of a recent investigation of the magnetic properties of A₂FeMoO₆ systems,^{16,20} where a pressure induced increase of T_C was observed. This comparison suggests that the electron-phonon interaction and the magnetic behavior of the system are not substantially coupled, thus supporting the theoretical approaches which neglect the role of the charge-lattice coupling in the magnetic mechanism.

¹I. Kobayashi, T. Kimura, H. Sawada, K. Terakura, and Y. Tokura, *Nature (London)* **395**, 677 (1998).

²D. D. Sarma, *Curr. Opin. Solid State Mater. Sci.* **5**, 261 (2001).

³G. A. Prinz, *Science* **282**, 1660 (1998); S. A. Wolf, D. D. Awschalom, R. A. Buhrman, J. M. Daughton, S. von Molnar, M. L. Roukes, A. Y. Chtchelkanova, and D. M. Treger, *ibid.* **294**, 1488 (2001).

⁴*Colossal Magnetoresistance Oxides*, Monographs in Condensed Matter Science, edited by Y. Tokura (Gordon and Breach, Reading, 2000).

⁵C. Ritter, M. R. Ibarra, L. Morellon, J. Blasco, J. Garcia, and J. M. De Teresa, *J. Phys.: Condens. Matter* **12**, 8295 (2000).

⁶D. D. Sarma, P. Mahadevan, T. Saha-Dasgupta, S. Ray, and A. Kumar, *Phys. Rev. Lett.* **85**, 2549 (2000).

⁷T. Saitoh, M. Nakatake, A. Kakizaki, H. Nakajima, O. Morimoto, Sh. Xu, Y. Morimoto, N. Hamada, and Y. Ayura, *Phys. Rev. B* **66**, 035112 (2002).

⁸T. Zhang, W. R. Brandford, H. J. Trodahl, A. Sarma, J. Rager, J. L. MacManus-Driscoli, and F. Cohen, *J. Raman Spectrosc.* **35**, 1081 (2004).

⁹C. de Francisco, J. M. Munoz, M. Zazo, A. G. Flores, J. Iniguez, and L. Torres, *J. Appl. Phys.* **89**, 7642 (2001).

¹⁰N. E. Massa, J. A. Alonso, M. J. Martinez-Lope, and M. T. Ca-

sais, *Phys. Rev. B* **72**, 214303 (2005).

¹¹P. Zaho, R. C. Yu, F. Y. Li, and Z. X. Liu, *J. Appl. Phys.* **92**, 1942 (2002).

¹²R. C. Yu, P. Zhao, F. Y. Li, Z. X. Liu, Z. Zhang, J. Liu, and C. Q. Jin, *Phys. Rev. B* **69**, 214405 (2004).

¹³U. Fano, *Phys. Rev.* **124**, 1866 (1961).

¹⁴M. V. Klein, in *Light Scattering in Solids I*, Topics Appl. Phys. Vol. 8, edited by M. Cardona (Springer, Berlin, 1983), p. 119.

¹⁵S. Ray, A. Kumar, S. Majumdar, E. V. Sampathkumaran, and D. D. Sarma, *J. Phys.: Condens. Matter* **13**, 607 (2001).

¹⁶D. Di Castro, P. Dore, R. Khasanov, H. Keller, D. D. Sarma, S. Ray, and P. Postorino (unpublished).

¹⁷P. Postorino, A. Congeduti, E. Degiorgi, J. P. Itie, and P. Munsch, *Phys. Rev. B* **65**, 224102 (2002).

¹⁸A. Congeduti, P. Postorino, E. Caramagno, M. Nardone, A. Kumar, and D. D. Sarma, *Phys. Rev. Lett.* **86**, 1251 (2001).

¹⁹C. C. Homes, T. Timusk, D. A. Bonn, R. Liang, and W. N. Hardy, *Can. J. Phys.* **73**, 663 (1995).

²⁰C. Goko, Y. Endo, E. Morimoto, J. Arai, and T. Matsumoto, *Physica B* **329**, 837 (2003).

²¹Y. Tomioka, T. Okuda, Y. Okimoto, R. Kumai, K. I. Kobayashi, and Y. Tokura, *Phys. Rev. B* **61**, 422 (2000).